On the Stable Passive Dynamics of Quadrupedal Running

Ioannis Poulakakis
poulakas@cim.mcgill.ca
Centre for Intelligent Machines
McGill University
3480 University, Montreal, H3A 2A7
Canada

Evangelos Papadopoulos
egpapado@central.ntua.gr
Dept. of Mechanical Engineering
National Technical University of Athens
Heroon Polytechniou 9, Athens, 15773
Greece

Martin Buehler
buehler@cim.mcgill.ca
Centre for Intelligent Machines
McGill University
3480 University, Montreal, H3A 2A7
Canada

Abstract - **In this paper, we study the passive dynamics of quadrupedal bounding, based on a simplified model of our Scout II quadruped robot. Surprisingly, numerical return map studies reveal that passive generation of a large variety of cyclic bounding motion is possible. Most strikingly, local stability analysis shows that the dynamics of the open loop passive system alone can confer stability of the motion! Stability improves at higher speeds, which is in agreement with recent results from biomechanics. These results can be used in developing a general control methodology for legged robots, resulting from the synthesis of feed-forward and feedback models that take advantage of the mechanical system, and might explain the success of simple, open loop bounding controllers on our experimental robot.**

I. INTRODUCTION

Mobility and versatility are the most important reasons for building legged robots, instead of wheeled and tracked robots, and for studying legged locomotion. Animals exhibit impressive performance in handling rough terrain and they can reach a much larger fraction of the earth landmass on foot than most of the existing wheeled vehicles. Most mobile robotic applications can benefit from the improved mobility and versatility that legs might offer.

Twenty years ago, Raibert set the stage with his groundbreaking work on legged robots by introducing a three-part controller, for stabilizing running on his one-, two-, and four-legged machines, [10]. His controllers, although very simple, resulted in high performance running with different gaits. Other research showed that even simpler control laws, which do not require task-level or torso-state feedback, can be used to stabilize running, [2]. Indeed, previous work on our quadruped robot Scout II (Fig. 1) showed that *open loop* control laws simply positioning the legs at a desired touchdown angle, result in high performance running at speeds up to 1.3 m/s, [12].

Similar results showing that complex full state feedback control laws may not be necessary to generate rhythmic motion have also been obtained in the context of biology and biomechanics. Pearson described experiments in animals, which show that the high level nervous system is not required for generating the rhythmic motions for walking, [8]. Therefore, one can assume that complex, neural equivalent control laws are not required to generate walking in animals. To explore the role of the mechanical system in control, Kubow and Full developed a simple two-dimensional dynamic model of a hexapedal runner (death-head cockroach, *Blaberous discoidalis*), [6]. The model had no equivalent of nervous feedback among any of its components and it was found to be inherently stable. This work first revealed the potential importance of *mechanical* feedback in simplifying neural control by demonstrating that stability could result from leg moment arm changes alone.
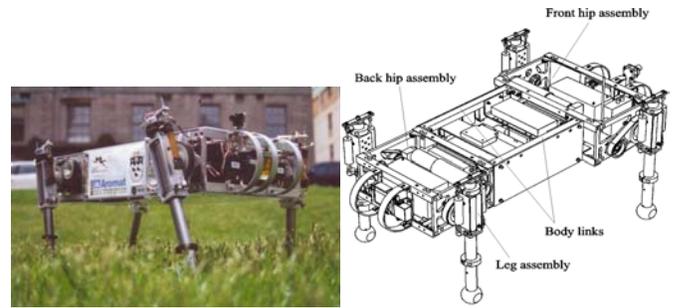
Fig. 1. Scout II: A high performance, autonomous four-legged robot.

In an attempt to set the basis for a systematic approach in studying legged locomotion, Full and Koditschek introduced the concept of *templates* and *anchors,* [5]. To study the basic properties of sagittal plane running, the *Spring Loaded Inverted Pendulum (SLIP)* template has been proposed, which describes running in animals that differ in skeletal type, leg number and posture, [5]. Recently, Seyfarth et. al., [11], and Chigliazza et al., [3], found that for certain touchdown angles, the SLIP becomes self-stabilized if the leg stiffness is properly adjusted and a minimum running speed is exceeded and they discovered that by increasing speed, the system becomes less sensitive to perturbations. Similar return map studies by Cham et. al. show that robustness can be achieved without sensory feedback but with a properly designed mechanical system [4].

In this paper, motivated by the recent results described above, we attempt to provide an explanation for simple control laws being adequate in stabilizing a complex task like quadruped running, based on a simple sagittal "template" model. Passively generated cyclic motions are identified based on a return map and a regime where the system is self-stabilized against perturbations is also found.

The practical motivation for studying the *passive dynamics* (defined as the unforced response of the system under a set of initial conditions) is threefold. First, if the system remains close to its passive behavior, then the actuators have less work to do to maintain the motion and energy efficiency, an important issue in mobile robots, is improved. Second, if there are operating regimes where the system is passively

stable, then active stabilization is not required or else will require less control effort and sensing. Finally, the passive dynamics of a system can be used as a design tool to specify desirable behavior of complex, underactuated dynamical systems, where reference trajectory tracking is not possible.

II. EXPERIMENTS WITH SCOUT II

Scout II has been designed for power-autonomous operation: The two hip assemblies contain the actuators and batteries, and the body houses all computing, interfacing and power distribution (Fig. 1). The mechanical design of Scout II is an exercise in simplicity. Besides its modular design, the most striking feature is the fact that it uses a *single* actuator per leg – the hip joint provides leg rotation in the sagittal plane. Each leg assembly consists of a lower and an upper leg, connected via a spring to form a compliant prismatic joint. Thus each leg has two degrees of freedom (DOF): the hip DOF (actuated), and the linear compliant DOF (passive).

In bounding, Scout uses its front and back legs in pairs, thus the essentials of the motion take place in the sagittal plane. According to the virtual leg concept, [10], the back and front physical legs can be replaced by single back and front virtual legs, respectively. The controller is based on two individual, independent leg controllers, without a notion of the overall body state. The front and back virtual legs each detect two leg states - stance and flight, which are separated by touchdown and lift-off events. There is no actively controlled coupling between the back and front legs – the bounding motion is purely the result of the controller interaction through the multi-body dynamic system. During flight, the controller servoes the flight leg to a desired, fixed, touchdown hip angle, then sweeps the leg during stance until a sweep limit, is reached**.** In the stance phase, a constant torque of 35 Nm is commanded at the hip (however, the actual applied torque is determined primarily by the motor's torque-speed limits, until the sweep limit is reached, [12]).

Scout II is an under-actuated, highly nonlinear, intermittent dynamical system. The complexity is further increased by the limited ability in applying hip torques due to actuator and friction constraints and by the existence of unilateral ground forces. Moreover, as Full and Koditschek state in [5], "locomotion results from complex high-dimensional, dynamically coupled interaction between an organism and its environment". Thus, the task itself is complex too, and cannot be specified via reference trajectories, or forward speeds. Despite this complexity, simple control laws can stabilize periodic motions, resulting in robust and fast running. Indeed, the controller described above does *not* require any task level feedback like forward velocity. Surprisingly, it also does *not* require body state feedback: one only needs to know the position of the leg with respect to the body and its state (flight or stance). It is therefore natural to ask why such a complex system can accomplish such a complex task via minor control action. As outlined in this paper, a possible answer is that Scout II's unactuated, conservative dynamics *already* exhibits stable bounding cycles, and hence a simple controller is all that is needed for keeping the robot bounding.

III. PASSIVE DYNAMICS OF BOUNDING

The template model for the passive dynamics of Scout II is shown in Fig. 2. Note that it can also be used to study other running gaits in the sagittal plane, like pronking. The goal of this analysis is to determine the conditions required to permit steady state cyclic motion of Scout II.
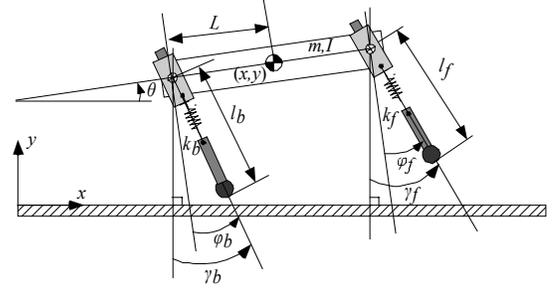
Fig. 2. A template for studying sagittal plane running on Scout II.

The controller presented in Section II is triggered by leg touchdown and liftoff events and results in the bounding gait presented in Fig. 3. Note that this bounding gait is different from the one studied in [1] and [10] in that there exists a phase where both the front and back legs are in stance (double leg stance). In each phase, the dynamic system equations are different since each of them is characterized by a different constraint set.

To derive a simplified mathematical model for Scout II, we assume massless legs. Also, a toe in contact with the ground is treated as a frictionless pin joint. In each phase, the equations of motion are

$$\frac{d}{dt}\begin{bmatrix} \mathbf{q} \\ \dot{\mathbf{q}} \end{bmatrix} = \begin{bmatrix} \dot{\mathbf{q}} \\ -\mathbf{M}^{-1}\left(\mathbf{V} + \mathbf{F}_{el} + \mathbf{G}\right) \end{bmatrix}, \qquad (1)$$

where $\mathbf{q} = [x \quad y \quad \theta]^T$, see Fig. 2, $\mathbf{M}$ is the mass matrix and $\mathbf{V}$, $\mathbf{F}_{el}$ and $\mathbf{G}$ are the vectors of the velocity dependent forces, the elastic and the gravitational forces respectively. The transition equations for touchdown and lift-off are

$$y \pm L\sin\theta \le l_0 \cos\gamma_i^{td}, \qquad (2a)$$

$$l_i^{lo} = l_0, \qquad (2b)$$

where $i = b, f$ for the back (- in (2a)) and front (+ in (2a)) virtual leg respectively. The complexity of the equations precludes finding the return map analytically, and therefore we must resort to a numerical evaluation of the return map.

To define the return map, we use the apex height in the double leg flight phase as a reference point since it allows for the touchdown angles to *explicitly* appear in the definition of the return map as kinematic inputs available for control. Therefore, we seek a function that maps the apex height of the nth stride to the apex height of the $(n+1)^{th}$ stride i.e. *the return map*. The states at the nth apex height constitute the initial conditions for the cycle, based on which we integrate the double flight phase equations, until the back leg touchdown event occurs. This event triggers the back leg stance phase, whose dynamic equations are integrated using as initial conditions the final conditions of the previous phase

(since massless legs are considered there are no impacts at touchdown).
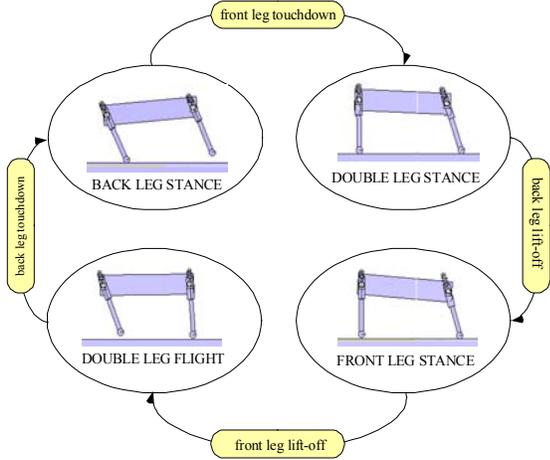
Fig. 3. Bounding phases and events.

Successive forward integration of the dynamic equations of all the phases yields the state vector at the $(n+1)^{th}$ apex height, which is the value of the return map calculated at the nth apex height. If the state vector at the new apex height is identical to the initial, then the cycle is repetitive. We seek such "re-entry" conditions, i.e. fixed points of the return map $\mathbf{P}: \mathbb{R}^4 \times \mathbb{R}^2 \to \mathbb{R}^4$,

$$\mathbf{x}_{n+1} = \mathbf{P}(\mathbf{x}_n, \mathbf{u}_n), \tag{3}$$

with $\mathbf{x} = \begin{bmatrix} y & \theta & \dot{x} & \dot{\theta} \end{bmatrix}^T$, $\mathbf{u} = \begin{bmatrix} \gamma_b^{td} & \gamma_f^{td} \end{bmatrix}^T$. Note that the touchdown angles are inputs available for control.

IV. PASSIVE BOUNDING CYCLES

We want to find an argument $\mathbf{x}$ in (3) that maps onto itself, i.e. we want to solve the equation

$$\mathbf{x} - \mathbf{P}(\mathbf{x}) = \mathbf{0}, \tag{4}$$

for all (experimentally) reasonable values of touchdown angles. Existence of solutions for (4) is not guaranteed, but seems to be the rule rather than the exception.

The search space is 4-dimensional with two free parameters, since for different values of touchdown angles, different solutions may be obtained. To describe $\mathbf{P}$ as a nonlinear function by analytically integrating the dynamic equations over this space is impossible. Thus the search is conducted numerically using the Newton-Raphson method, where an initial guess, $\mathbf{x}_n^{\langle 0 \rangle}$, for the fixed point is assumed and then updated using the equation

$$\mathbf{x}_n^{\langle k+1 \rangle} = \mathbf{x}_n^{\langle k \rangle} + \left(\mathbf{I} - \nabla \mathbf{P}(\mathbf{x}_n^{\langle k \rangle}) \right)^{-1} \left[\mathbf{P}(\mathbf{x}_n^{\langle k \rangle}) - \mathbf{x}_n^{\langle k \rangle} \right], \tag{5}$$

where n corresponds to the nth apex height and k corresponds to the number of iterations.

To find a solution we evaluate (5) iteratively until convergence (the error between $\mathbf{x}_n^{\langle k \rangle}$ and $\mathbf{x}_n^{\langle k+1 \rangle}$ is smaller than $1e-6$). The value of $\mathbf{P}$ at $\mathbf{x}_n^{\langle k \rangle}$ is calculated through the numerical integration of the dynamic equations (the adaptive

step Dormand-Price method was used with $1e-6$ and $1e-7$ relative and absolute tolerances, respectively) during a complete cycle. Since central difference approximation is used to evaluate numerically the Jacobian of the return map, each iteration involves nine evaluations of the return map $\mathbf{P}$. Evaluating (5) is computationally intensive, however, if the initial guess is reasonable and a solution exists, this method finds it usually in less than eight iterations.

Surprisingly, using the above method we were able to find many fixed points of the return map $\mathbf{P}$, for different initial guesses and different touchdown angles. All these fixed points exhibited some very useful properties concerning the symmetry of the bounding motion. In Fig. 4 plots showing the evolution of the states during one cycle of the bounding motion corresponding to a fixed point are presented. It is apparent that the pitch angle θ is zero at the apex height. This property has been observed for all the fixed points found.
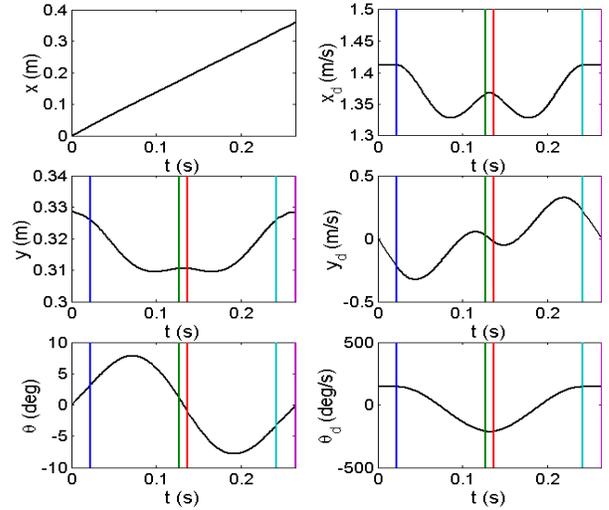
Fig. 4. Evolution of the state variables during one bounding cycle, corresponding to a fixed point. The vertical lines show the events.

Fig. 5 presents the leg lengths and the leg angles for the back and front virtual legs during one cycle and for the fixed point of Fig. 4. Careful inspection of Fig. 5 reveals another important property of the fixed points. It can be seen that the touchdown angle of the front leg is equal to the negative of the lift-off angle of the back leg while the touchdown angle of the back leg is equal to the negative of the lift-off angle of the front leg i.e.

$$\gamma_f^{td} = -\gamma_b^{lo}, \; \gamma_b^{td} = -\gamma_f^{lo}. \tag{6}$$

As shown in Figs. 4 and 5, the passively generated bounding motion exhibits symmetric properties about the middle of the double stance phase. This is always true for all the fixed points found randomly by following the method described above. It is interesting to note that in the case of the SLIP model, a necessary and sufficient condition for fixed points is the symmetric stance phase, i.e. the lift-off angle is equal to the negative of the touchdown angle [3]. We will use this property to derive a more systematic searching procedure

for finding fixed points at specific forward speeds and apex heights.
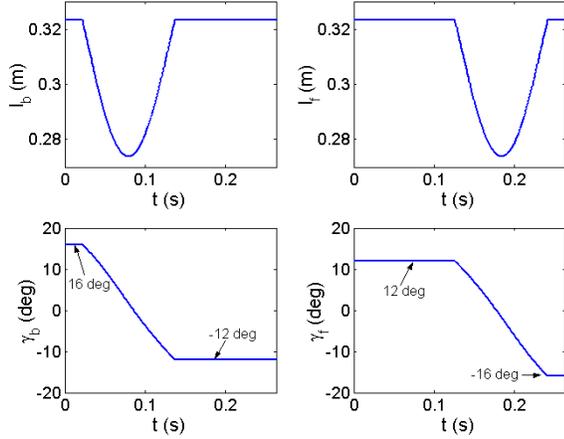
Fig. 5. Evolution of the leg length and angle.

V. CONTINUUMS OF FIXED POINTS

For Scout II's bounding running, a specific horizontal speed at apex and a sufficient apex height that prevents toe stubbing are useful functional requirements. Therefore, the scheme described above is modified here so that the forward speed and apex height become its input parameters, specified according to running requirements, while the touchdown angles are now considered to be "states" of the searching procedure, i.e. variables to be determined from it. By doing so, the *search space* states and the vector of the parameters ("inputs" to the search scheme) are respectively

$$\mathbf{x}^* = \begin{bmatrix} \theta & \dot{\theta} & \gamma_b^{td} & \gamma_f^{td} \end{bmatrix}^T, \quad \mathbf{u}^* = \begin{bmatrix} y & \dot{x} \end{bmatrix}^T. \qquad (7)$$

It is important to mention that the numerical integration of the equations of motion starting from the apex height event, results in the calculation of lift-off angles and *not* of the touchdown angles of the legs at the next apex height event. This is a direct consequence of the assumption of massless legs. Thus, to calculate the gradients needed to implement the Newton-Raphson scheme, the lift-off angles must be "mapped" to touchdown angles based on the symmetry described by (6). Then, by using the Newton-Raphson algorithm, we update the initial guess until convergence is achieved (for more details see [9]).

Note that the above search scheme does not explicitly ensure that

$$y_{n+1} = y_n, \quad \dot{x}_{n+1} = \dot{x}_n, \qquad (8)$$

which is a consequence of the definition of a fixed point. Instead, in the new search scheme, we required that (6) holds. However, examination of the search results shows that the conditions described by (8) are also satisfied. This numerical fact shows that the conditions described by (6) are equivalent to the conditions for the existence of a fixed point. Note that this behavior is analogous to that of the SLIP, where the symmetric stance phase is a condition for a fixed point, [3].

Fig. 6 displays fixed points for 1 m/s forward speed, 0.35 m apex height and varying pitch rate. It can be seen that there is a continuum of fixed points, which follows an "eye" pattern, accompanied by two external branches. The existence of the external branch means that there is a range of pitch rates where two *different* fixed points exist for the same forward speed, apex height and pitch rate. This is quite surprising since the same total energy and the same distribution of that energy among the three modes of the motion --forward, vertical and pitch-- results in two different motions depending on the touchdown angles. As it can be seen from Fig. 6, the fixed points that lie on the internal branch correspond to a bounding motion where the front leg is brought in front of the torso, while the fixed points that lie on the external branch correspond to a motion where the front leg is brought towards the torso's Center of Mass (COM).
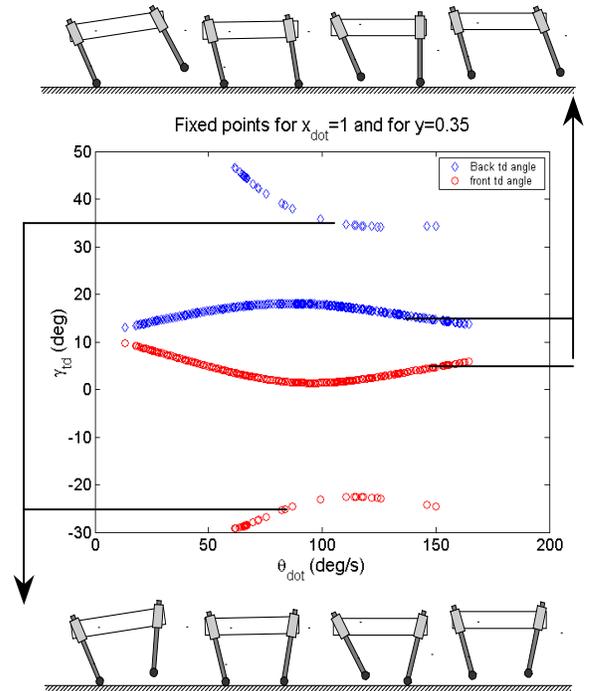
Fig. 6. Fixed points for 1m/s forward speed and 0.35 m apex height. Snapshots show the motions corresponding to the fixed points.

Fig 7 presents fixed points for forward speeds varying from 1.5 to 4 m/s and for a 0.35 m constant apex height. It can be seen that at higher speeds, the "eye" pattern shifts to higher values of the touchdown angles, i.e. larger touchdown angles are required to maintain higher speeds, a fact which is in agreement with Raibert's findings, [10]. No external branches of fixed points at speeds higher that 1 m/s were found. Note that the fixed points shown in Fig. 7 correspond to different energy ranges, which do not overlap, a fact that is particularly important for designing controllers since it shows that different speeds require different energies, see [9] for more details. Therefore, an energy-tracking controller is necessary.

In reading Figs. 6 and 7, it is useful to note that the region close to the vertical axis corresponds to pronking-like motions. Indeed, recall that, at the apex height $\theta = 0$ always,

(see Fig. 4 in Section IV). As we approach the vertical axis of Figs. 6 and 7 ($\dot{\theta} = 0$), the touchdown angles of the front and back legs tend to become equal. A gait with $\theta = 0$, $\dot{\theta} = 0$ and equal touchdown angles for the front and back legs corresponds to the pronking gait, where the front and back legs strike the ground almost in unison. Therefore, points near the vertical axis correspond to pronking-like motions. Useful conclusions concerning the stability of the bounding and the pronking gaits will be discussed in the next section.
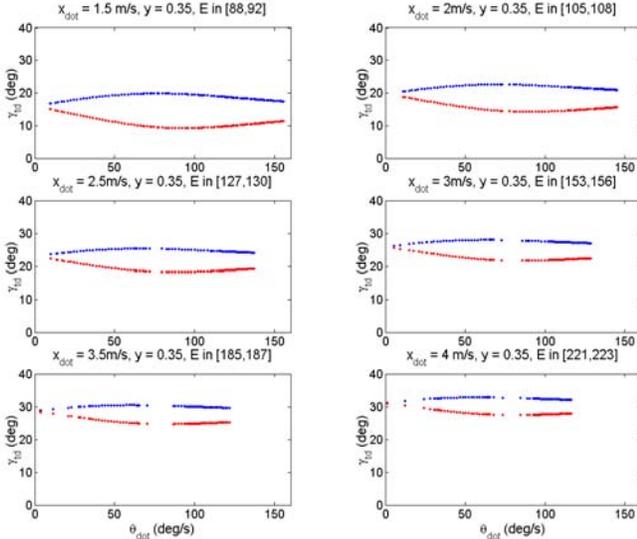
Fig. 7. Fixed points for a 0.35 m apex height and speeds from 1.5 to 4 m/s. E is the total energy.

VI. STABILITY OF PASSIVE BOUNDING

The existence of passively generated bounding running cycles is by itself a very important result since it shows that an activity as complex as running can simply be a natural motion of the system. However, in real situations the robot is continuously perturbed, therefore, if a fixed point were unstable, then the periodic motion would not be sustainable. In this section, we characterize the stability of the fixed points found in Section V using local stability analysis.

To investigate stability, we assume that the apex height states are perturbed from their steady-cycle values $\overline{\mathbf{x}}$, by some small amount $\Delta \mathbf{x}$. The discrete model that relates the deviations from steady state is

$$\Delta \mathbf{x}_{n+1} = \mathbf{A}\Delta \mathbf{x}_n + \mathbf{B}\Delta \mathbf{u}_n , \qquad (9)$$

where $\Delta \mathbf{x} = \mathbf{x} - \overline{\mathbf{x}}$, $\Delta \mathbf{u} = \mathbf{u} - \overline{\mathbf{u}}$. For small perturbations, the apex height states at the next stride can be calculated by the linear difference equations (9). If all the eigenvalues of the system matrix $\mathbf{A}$ have magnitude less than one, then the periodic solution is stable.

Fig. 8 shows the eigenvalues of matrix $\mathbf{A}$ for forward speed 1 m/s and apex height 0.35 m and varying pitch rate. Note that the same pattern is observed for different forward speeds and apex heights. As it was expected, one of the eigenvalues is always located at one, representing the fact that the system is conservative. Two of the eigenvalues start on the real axis, and as $\dot{\theta}$ increases they move towards each

other, they meet on the real axis and finally they move towards the rim of the unit circle. The third eigenvalue starts at a high value and moves towards the unit circle but it never gets into it, for those specific values of forward speed and apex height. Therefore there is no region of parameters where the system is passively stable for speed $\dot{x} = 1 m / s$ and apex height $y = 0.35 m$.
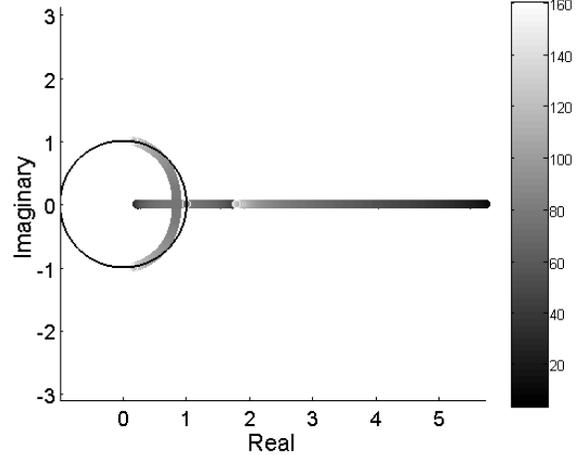
Fig. 8. Root locus showing the paths of the four eigenvalues as the pitch rate increases.

To show how the forward speed and the apex height affect the stability of the motion we present Figs 9 and 10. Fig. 9 shows the magnitude of the larger eigenvalue at different forward speeds. For sufficiently high forward speeds and pitch rates, the larger eigenvalue enters the unit circle while the other two eigenvalues remain well behaved. Therefore, there exists a regime where the system can be passively stable. This is a very important result since it shows that the system can tolerate small perturbations of the nominal conditions *without* any control action taken! This fact could provide a possible explanation to why our Scout II robot can bound, without the need of complex state feedback. It is important to mention that this result is in agreement with recent research from biomechanics, which shows that when animals run at high speeds, passive dynamic self-stabilization from a feed-forward, tuned mechanical system can reject rapid perturbations and simplify control [5], [6]. Analogous behavior has been discovered by McGeer in his passive bipedal running work, [7], and recently in the SLIP template, [3], [11].

Fig. 10 shows how the norm of the maximum eigenvalues changes as a function of the pitch rate, at different apex heights, keeping the forward speed constant at 3 m/s. It can be seen that the lower the apex height is, the less unstable the system is. Therefore, greater forward speeds and lower apex heights contribute to the stability of the open loop system. This fact has been observed in both simulations and experiments, where for a given energy level, the system stabilizes itself at high pitch rates and low apex heights.

It is important to note that, as depicted in all the above plots (Figs. 8, 9 and 10), the largest eigenvalue obtains its

maximum value when the pitch rate $\dot{\theta}$ is small. Recall that the region where $\dot{\theta}$ takes small values corresponds to a pronking-like motion, where both the front and back legs hit and leave the ground in unison. Thus, we can conclude that pronking-like motions (low-pitch rates) are more unstable than bounding, (high pitch rates). This behavior can be explained based on the concept of the dimensionless moment of inertia j, developed by Murphy and Raibert [10],

$$ j = \frac{I}{mL^2} , \tag{10} $$

where I, m, and L are defined in Fig. 2. Based on simulations, Raibert and Murphy found that when $j < 1$ the torso rotates easier (high-pitch rates) than it translates (low-pitch rates), resulting to bounding motions, [10]. For an analytical proof of this observation, see [1]. For Scout II, $j = 0.742$, thus pronking is not a natural gait for Scout II when efficient, high-speed locomotion is needed [9].
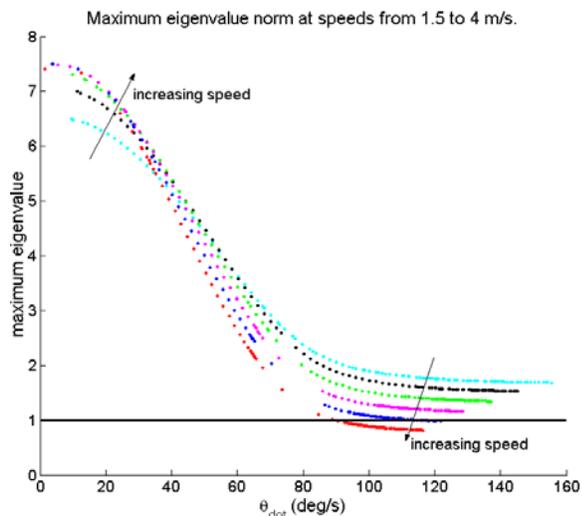
Fig. 9. Largest eigenvalue norm at various pitch rates and for forward speeds between 1.5 and 4m/s. The apex height is 0.35 m.
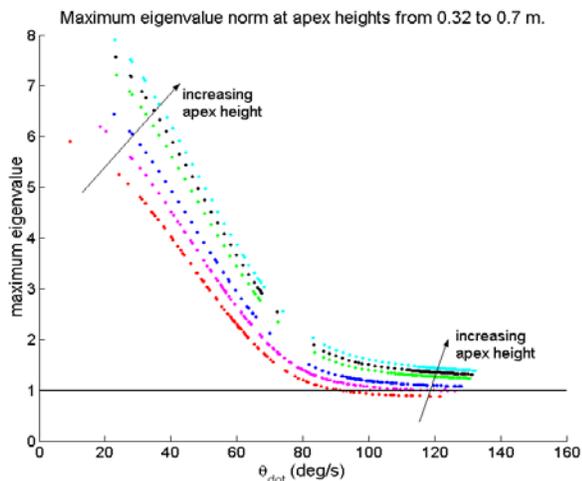
Fig. 10. Largest eigenvalue norm at various pitch rates and for apex heights from 0.32 to 0.37m. The forward speed is 3m/s.

VII. CONCLUSION

In this paper we studied the passive dynamics of the bounding running gait of a simple conservative (energy preserving) model of our Scout II robot. Based on the analysis of a numerically derived return map, we found that the bounding cycle can be passively generated with appropriate initial conditions. Moreover, there exists a regime where the model stabilizes itself without the need of any control action. This might explain why simple controllers, as reported in [12], are adequate in stabilizing a complex dynamic task like quadruped running. Also, these results are in agreement with recent results from biomechanics. Self-stabilization can facilitate the design of control laws for dynamically stable legged locomotion by designing controllers that expand the domain of attraction of that behavior. These controllers are currently under investigation.

VIII. ACKNOWLEDGMENTS

IX. REFERENCES

[1] Berkemeier M. D., "Modeling the Dynamics of Quadrupedal Running", in *The Int. J. of Robotics Research*, Vol. 17, No 9, pp. 971-985, 1998.

[2] Buehler M., "Dynamic Locomotion with One, Four and Six-Legged Robots", in *J. of the Robotics Society of Japan*, 20 (3), pp. 15-20, 2002.

[3] Chigliazza R. M., Altendorfer R., Holmes P. and Koditschek D. E., "Passively Stable Conservative Locomotion", submitted to *SIAM J. of Applied Dynamical Systems*.

[4] Cham J. G., Bailey S. A. and Cutkosky M. R., "Robust Dynamic Locomotion through Feedforward - Preflex Interaction", in *ASME Int. Mechanical Engineers Congress and Exposition (IMECE)*, Orlando, FL, 2000.

[5] Full R. J. and Koditschek D., "Templates and Anchors: Neuromechanical Hypotheses of Legged Locomotion on Land", in *J. of Experimental Biology*, 202, pp. 3325-3332, 1999.

[6] Kubow T. and Full R., "The Role of the Mechanical System in Control: A Hypothesis of Self-stabilization in Hexapedal Runners" in *Phil. Trans. of the Royal Society of London Series B – Biological Sciences* 354 (1385), pp. 854-862, 1999.

[7] McGeer T., "Passive Bipedal Running", *Technical Report, CSS–IS TR 89-02*, Simon Fraser University, Centre For Systems Science, Burnaby, BC, Canada, 1989.

[8] Pearson K., "The Control of Walking", *Scientific American*, Vol. 72, pp. 86, 1976.

[9] Poulakakis I., *On the Passive Dynamics of Quadrupedal Running*, M. Eng. Thesis, McGill University, Montreal, QC, Canada, July 2002.

[10] Raibert M. H., *Legged Robots that Balance*, MIT Press, Cambridge MA, 1986.

[11] Seyfarth A., Geyer H., Guenther M. and Blickhan R., "A Movement Criterion for Running", in *J. of Biomechanics*, Vol. 35, pp. 649-655, 2002.

[12] Talebi S., Poulakakis I., Papadopoulos E. and Buehler M., "Quadruped Robot Running with a Bounding Gait" in *Experimental Robotics VII*, D. Rus and S. Singh (Eds.), pp. 281-289, Springer-Verlag, 2001.